Stochastic Ship-radiated Noise Modelling via Generative Adversarial Networks

Lazar Atanackovic[†], Vala Vakilian*[†], Dryden Wiebe*[†], Lutz Lampe[†], and Roee Diamant[§]

[†]Department of Electrical and Computer Engineering, University of British Columbia, Canada
[§]Department of Marine Technologies, University of Haifa, Israel
Corresponding author, email: *lazaratan@ece.ubc.ca*
(*equal contribution)

***Abstract*—The design and performance evaluation of underwater acoustic (UA) communication systems in shallow water and harbour environments is a continuous challenge due to the numerous degrading factors present in the UA channel, one of which is the presence of noise generated due to nearby shipping activity. However, few research studies have examined the properties of ship-radiated noise in terms of its time-domain statistical characteristics and its negative effects on UA communication systems. We propose the use of unsupervised learning techniques to train generative models that capture the time-domain stochastic behaviours of ship-radiated noise using a publicly available database of long-term acoustic shipping noise recordings. These models can then be used for further analysis of ship-radiated noise and performance evaluation of UA orthogonal frequency-division multiplexing systems in the presence of such interference. For further validation, we include experimentally acquired ship-radiated noise recordings acquired off the coast of Caesarea, Israel. The results indicate a two component Gaussian mixture model serves as a better approximation for high frequency ship-radiated noise while generative adversarial networks produce improved realizations of shipping noise in lower frequencies.**

***Index Terms*—Generative adversarial network (GAN), Gaussian mixture model (GMM), orthogonal frequency-division multiplexing (OFDM), ship-radiated noise.**

I. Introduction

The underwater acoustic (UA) channel introduces significant linear and nonlinear distortions as well as additive perturbations to a communication signal [1]. Among the latter, ship-radiated noise is a major contributor in harbour and shallow water environments, limiting the data rate performance and reliability of UA communication systems. There have been various studies that explore the spectral and ambient characteristics associated with shipping activity in the UA channel [2]–[6]. However, the development of a stochastic model for ship-radiated noise has not received much attention. The lack of an adequate stochastic noise model introduces challenges when designing and evaluating the performance of high data rate communication for implementation in the presence of such interference. In this work, we focus on the challenge of producing a time-domain probabilistic model for ship-radiated noise.

Gaussian mixture models (GMMs) are a well known stochastic model used in evaluating the performance of UA communication systems in the presence of impulse noise [7]. Recent work in [8] postulates the use of GMMs to temporally describe the statistical and impulsive behaviour of ship-radiated noise. The GMM serves well in modelling some of the probabilistic and impulsive properties of high frequency (HF) ship-radiated noise, but does not capture existing correlative structure, as in the case of low frequency (LF) noise. Therefore, producing a probabilistic model that can fully capture the varying properties and structure of ship-radiated noise remains a challenge.

Generative adversarial networks (GANs) are another popular generative modelling approach. Different from the GMM, which is trained via the expectation-maximization (EM) algorithm [9, Chapter 11], GANs train a generative model through a min-max two player game [10]. Since their original introduction, extensive research interest in probabilistic generative modelling via GANs has led to numerous variants of the GAN model. For instance, the deep convolutional generative adversarial network (DCGAN) [11], the conditional GAN [12], and the stacked GAN [13] are some examples of GAN model variants derived from the original adversarial training framework of the GAN model.

Recently, GANs [10] have shown growing success in producing probabilistic generative models for images and has sparked motivation in the field of communications for use in stochastic channel modelling. For instance, the authors in [14] propose an end-to-end learning communication system framework using a conditional GAN to model the stochastic channel effects, where the gradients of the end-to-end training procedure are propagated through the GAN. Likewise, [15] suggests the use of variational GANs for modelling a wide variety of stochastic channel effects learned from observed data. To this end, there is reason to believe that GANs can capture the stochastic behaviour and statistical characteristics of ship-radiated noise.

GAN models for applications in UAs have been proposed for acoustic signal identification [16] [17] and sonar imaging [18] [19]. However, to the best of our knowledge there have been no appearances in recent research that propose GAN based channel modelling approaches for UA communication systems. Due to the strenuous and unpredictable conditions of the UA channel, GANs may serve as viable solution for modelling UA stochastic channel behaviours when there is

This work is supported by the NATO Science for Peace and Security Programme under grant G5293.

access to data representative of the channel effects. Therefore, in this work we address the aforementioned research gap and provide the first attempt in using GANs for modelling ship-radiated channel noise.

Stimulated by the lack of an adequate temporal stochastic model for shipping noise, we propose the use of the DCGAN [11] to capture the correlative structure of LF ship-radiated noise, while investigating the suitability the GMM for modelling HF ship-radiated noise. We consider the implication of ship-radiated noise on orthogonal frequency-division multiplexing (OFDM) systems, thus we model ship-radiated noise in the equivalent complex baseband representation. Similar to [8], we conduct a data driven study utilizing the Ocean Networks Canada (ONC) publicly available database of long term acoustic recordings of shipping noise [20], to train a DCGAN that can generate new realistic realizations of ship-radiated noise. Likewise, with the ONC database, we use the EM algorithm to fit a GMM that provides a stochastic model for ship-radiated noise. We then evaluate the suitability of the GMM and the DCGAN in producing stochastic time-domain models of ship-radiated noise in the HF and LF band systems.

The remainder of this manuscript is organized as follows. In Section II, we introduce the OFDM system model, the GMM, and the data acquisition procedures. Then, the GAN for the stochastic modelling of ship-radiated noise is presented in Section III. In Section IV we present and discuss the numerical results regarding the performance evaluations of the respective generative models. Final concluding remarks are drawn are in Section V.

II. Methodology and Model Overview

We consider an OFDM system for data transmission and reception in the presence of ship-radiated noise. Our goal is to produce a time-domain stochastic model that can capture the statistical and correlative structure of ship-radiated noise interference while emulating OFDM signal reception. In this section we introduce the OFDM system model, the two component GMM, and the data acquisition and pre-processing procedures.

A. OFDM System Model

OFDM is a multi-carrier transmission technique which partitions the total bandwidth W into N individual sub-channels each separated by a narrow frequency interval $\Delta f = W/N$, ultimately leading to transmission rates that are close to channel capacity. Each OFDM sub-channel may be individually modulated and coded, thus by denoting the complex-valued information symbols at each independent sub-channel as $x[k]$, where $k = 0, 1, ..., N-1$, the time-domain complex baseband transmission signal is expressed as

$$d(t) = \frac{1}{\sqrt{N}} \sum_{k=0}^{N-1} x[k] e^{j2\pi kt/T}, \qquad 0 \leq t \leq T \tag{1}$$

where $T = 1/\Delta f$ is the symbol duration. Likewise, equation (1), which utilizes the inverse discrete Fourier transform (IDFT), can be defined as a linear system

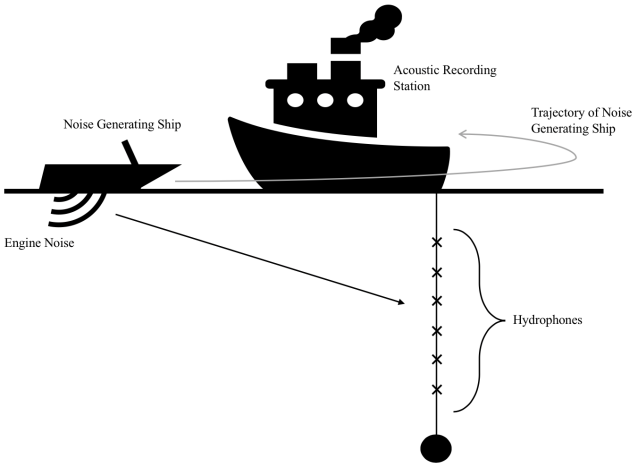

Fig. 1: Experimental set-up for acoustic acquisition of ship-radiated noise recordings.

$$\boldsymbol{d} = \boldsymbol{F}^H \boldsymbol{x} \tag{2}$$

where $\boldsymbol{d}$ is the discrete time data transmission vector and $\boldsymbol{F}^H$ is the IDFT matrix, with $(\cdot)^H$ defining the Hermitian transpose. The OFDM signal reception process is reverse to the transmission steps as defined by equation (1), using the DFT to re-acquire the transmitted symbols $x[k]$.

B. Gaussian Mixture Model

The previous work [8] shows the applicability of a two component complex circularly symmetric GMM in modelling the impulsive attributes of HF ship-radiated noise, and is denoted as

$$f(\boldsymbol{w}; \rho, \sigma_n^2, \tilde{\sigma_i}^2) = (1-\rho)\mathcal{NC}(\boldsymbol{w}; 0, \sigma_n^2) + \rho\mathcal{NC}(\boldsymbol{w}; 0, \tilde{\sigma_i}^2) \tag{3}$$

where $\mathcal{NC}$ is the complex normal distribution, $\tilde{\sigma_i}^2 = \sigma_n^2 + \sigma_i^2$ is the impulse noise variance, σ_n^2 is the background noise variance, and $0 \leq \rho \leq 1$ is the sparsity rate of the impulses. The GMM is trained in an unsupervised learning fashion using the iterative EM algorithm [9, Chapter 11]. Different from [8], we provide a more thorough evaluation the GMM for modelling the statistical and impulsive properties of ship-radiated noise. In addition, the GMM is evaluated and compared alongside the GAN-based generative model in terms of producing new realistic realizations of ship-radiated noise.

C. Data Acquisition and Pre-processing

The ONC data is collected identical to the procedure outlined in [8, Section II-C]. In addition to the ONC data, we include experimental ship-radiated noise acoustic recordings acquired through a set of sea trials off the coast of Caesarea, Israel, over a two day period of May 20^{th} and May 21^{st}, 2019. We use the experimentally acquired acoustic shipping

TABLE I: Acoustic recording pre-processing frequency bands

	Center Frequency	Bandwidth	LPF Cut-off
Low Frequency	2 kHz	4 kHz	2 kHz
High Frequency	12 kHz	8 kHz	4 kHz

noise recordings for further test validation of the DNN models for structured signal recovery.

The experimental set-up for the acquisition of acoustic shipping noise recordings is presented in Fig 1. We use a linear array of 6 hydrophones placed at approximately equal spacing over 10 meters of length with the first hydrophone starting at a depth of approximately 15 meters. The "noise generating ship" follows a continuous elliptical trajectory around the acoustic recording station, situated on the primary ship, producing acoustic ship-radiated noise, as shown in Fig 1. The experimental data acquisition procedure is outlined as follows:

1) With the "noise generating ship", we encircle the main ship in an elliptical trajectory and begin the acoustic recording via the linear hydrophone array. This step is carried out for approximately 1 minute in duration.
2) We record the time of day of the acoustic recording, later used to filter and find relevant data files.

We repeat Steps 1 and 2 at several occasions to gather an assortment of acoustic ship-radiated noise recordings over the duration of the 2 day sea trial. After carrying out numerous experimental trials, we identify the acoustic recordings with the most prominent ship-radiated noise and with minimal interference from other noise sources. Two experimental recordings of approximately one minute in length are identified and considered for analysis:

- **Acoustic recording 1**: Date: May 20th, Time: 15:52 – Label: EXP1
- **Acoustic recording 2**: Date: May 20th, Time: 15:53 – Label: EXP2

The ONC and experimental acoustic recordings are pre-processed such that signal reception in the OFDM system is emulated. We down-convert and low pass filter (LPF) the ONC and experimental shipping noise data. We consider HF and LF OFDM systems of 1024 sub-carriers at center frequencies of $f_c = 12$ kHz and $f_c = 2$ kHz with bandwidths of 8 kHz and 4 kHz, respectively (see Table I).

III. Generative Adversarial Network for Modelling Ship-radiated Noise

GANs directly learn the distribution of a given set of training example without any assumption or definition of the probability distribution function (PDF) of the data [10]. In contrast, the GMM first assumes the data follows a Gaussian mixture PDF, then fits the model parameters via the EM algorithm. Therefore, the GAN is desirable in the case where it is difficult to assume that a Gaussian PDF can probabilistically approximate the data. For instance, the case of LF ship-radiated noise, which is found to be less well characterized by the GMM [8]. In this section, we first present the general GAN model framework and introduce the iterative min-max GAN training process. Then, we present the DCGAN model for stochastic ship-radiated noise modelling.

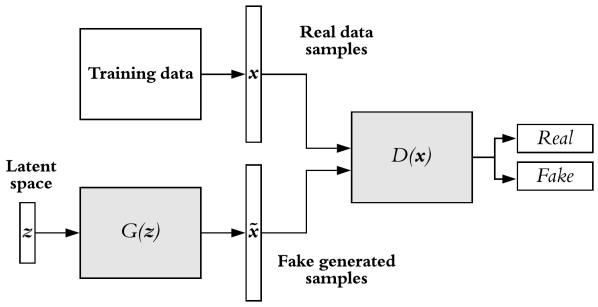

Fig. 2: General GAN structure.

A. Generative Adversarial Network

During training, GANs play a min-max two player game between the generator network G, which aims to generate new realistic and artificial instances of the training data, and a discriminator network D, which attempts to differentiate between real and fake data examples [10]. Let us denote the real training data examples as $\boldsymbol{x}$, the fake generated data examples as $\tilde{\boldsymbol{x}}$, and the latent space as $\boldsymbol{z}$. The generator network tries to learn an approximate distribution over the training data examples $\boldsymbol{x}$ by mapping a randomly generated low-dimensional latent space $\boldsymbol{z}$, drawn from some *prior* distribution $p(\boldsymbol{z})$, i.e. $\tilde{\boldsymbol{x}} = G(\boldsymbol{z})$. We sample the latent space $\boldsymbol{z}$ from a standard normal distribution, i.e. $\boldsymbol{z} \sim \mathcal{N}(\mu, \sigma^2)$, where $\mu = 0$ and $\sigma^2 = 1$. The discriminator network takes the real training data examples and the newly generated fake data examples as input and attempts to determine whether a certain example is drawn from the training set or generated from G. We illustrate this process in Fig 2. The two stages of the min-max training objective can be summarized:

- Train D such that the probability $D(\boldsymbol{x})$ of classifying the real and fake data examples is maximized.
- Train G such that the cost function $\log(1 - D(G(\boldsymbol{z})))$ is minimized.

Likewise, following from the two objectives listed above, we can denote the GAN objective function as

$$\min_G \max_D \{\mathbb{E}_{\boldsymbol{x}}[\log D(\boldsymbol{x})] + \mathbb{E}_{\boldsymbol{z}}[\log(1 - D(G(\boldsymbol{z})))]\} \ . \quad (4)$$

The training procedure iterates between maximizing $D(\boldsymbol{x})$ by fixing G, then minimizing $\log(1 - D(G(\boldsymbol{z})))$ by fixing D, until some convergence is achieved.

B. Deep Convolutional GAN

The DCGAN has shown success in generating sharp and realistic two dimensional images for various image data sets by embedding the architecture of convolutional neural networks (CNNs) within the GAN model framework [11]. Due to the

success of the DCGAN in probabilistically generating new realizations of images, we adopt the DCGAN for the task of stochastic ship-radiated noise modelling under a image processing framework. However, unlike typical implementations of the DCGAN for two dimensional images, we devise an alternate implementation for generating one dimensional complex vectors of ship-radiated noise signals. We utilize the complex number operations for deep neural networks (DNNs) to train two real number networks in parallel that capture the mathematical dependencies between the real and imaginary components [21]. Fig 3 (a) and Fig 3 (b) illustrate the respective single real number generator and discriminator networks of the DCGAN for ship-radiated noise modelling. Below we denote the structures of the generator and discriminator networks:

- **Generator network:** The general structure of the generator network is shown in Fig 3 (a). Let us denote $\boldsymbol{z}$ as the complex standard normal generated latent space vector. We use a latent space size of 64, thus the latent space layer of the DCGAN model is 64×1. The generator network consists of the four transposed convolutional hidden layers L_1, L_2, L_3, and L_4, which map the randomly generated 64×1 latent space vector $\boldsymbol{z}$ to a 1024×1 output vector $\tilde{\boldsymbol{x}}$. The dimensions of each layer are defined as $(n \times 1 \times k)$, where $n \times 1$ is the feature map size (the length of the one dimensional vectors) and k is the number of feature maps. The output vector $\tilde{\boldsymbol{x}}$ is the newly generated ship-radiated noise signal that probabilistically mimics the training data examples. The filter size of each transposed convolutional layer is 4×1. We use a stride of 2 and zero padding of 1 at each transposed convolutional layer. The rectified linear unit (ReLU) activation function is placed after the outputs of hidden layers L_1, L_2, and L_3 and the hyperbolic tangent activation function is used at the output layer L_4. Batch normalization layers are utilized at each hidden layer to aid in the convergence of the training process.
- **Discriminator network:** The general structure of the discriminator network is shown in Fig 3 (b). The discriminator network comprises five convolutional hidden layers that provide a mapping for determining whether a 1024×1 input vector is a real ship-radiated noise example or a fake example generated by the generator network. The five convolutional hidden layers L_1, L_2, L_3, L_4, and L_5 map the input vector to a single probability $D(\boldsymbol{x})$. For the discriminator network, we use a filter sizes of 4×1, a stride of 4, and zero padding of 1 at each convolutional hidden layer. The leaky ReLU activation function with the default α value is utilized at layers L_1, L_2, L_3, and L_4 and the sigmoid activation function is used at the output layer L_5. Identical to the generator network, we use batch normalization layers at each hidden layer to help in the convergence of the training process.

The activation function utilized in the DCGAN model are outlined in Table II.

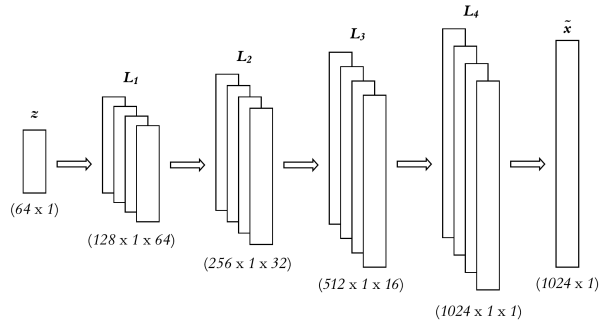

(a)

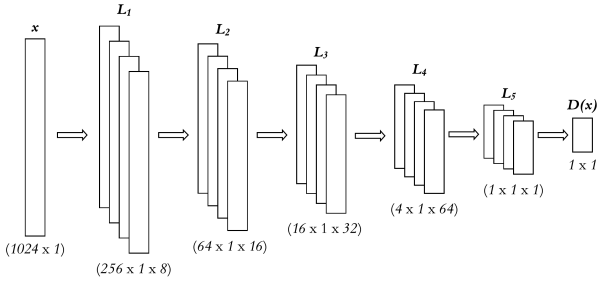

(b)

Fig. 3: DCGAN [11] for stochastic modelling of ship-radiated noise with (a) the generator network G, and (b) the discriminator network D.

TABLE II: Activation functions for transformations in DNNs.

Activation Name	Abbreviation	Function
Identity	–	$h(z) = z$ (5)
Rectified linear unit	ReLU(z)	$h(z) = \begin{cases} 0 & \text{for } z \leq 0, \\ z & \text{for } z > 0 \end{cases}$ (6)
Leaky rectified linear unit	LReLU(z)	$h(z) = \begin{cases} \alpha z & \text{for } z \leq 0, \\ z & \text{for } z > 0 \end{cases}$ (7) where $\alpha < 1$ (default value: $\alpha = 0.01$)
Sigmoid function	$\sigma(z)$	$h(z) = \dfrac{1}{1+e^{-z}}$ (8)
Hyperbolic tangent function	tanh(z)	$h(z) = \dfrac{e^{z}-e^{-z}}{e^{z}+e^{-z}}$ (9)

IV. Numerical Results

In this section, we present the numerical results of the DCGAN and GMM stochastic models for HF and LF ship-radiated noise. We consider three methods of evaluation to determine the suitability of the respective generative models for modelling the time-domain stochastic behaviour of shipping noise:

1) The 1-nearest neighbour (1-NN) two sample test, reporting the leave-one-out (LOO) accuracy in classifying the

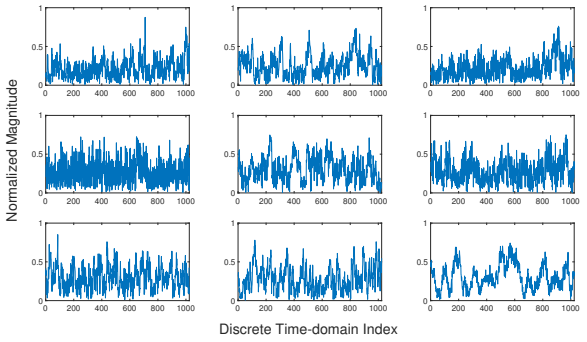

(a)

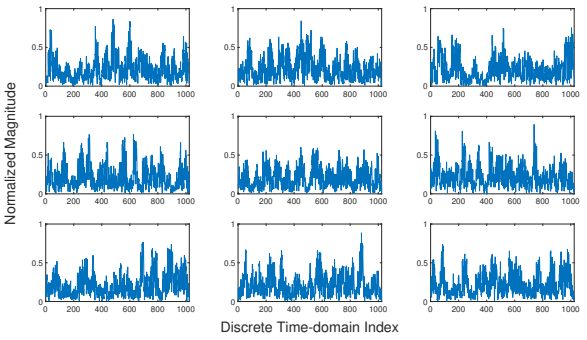

(b)

Fig. 4: LF Ship-radiated noise samples (a) real data examples, and (b) fake data examples generated via the LF DCGAN model.

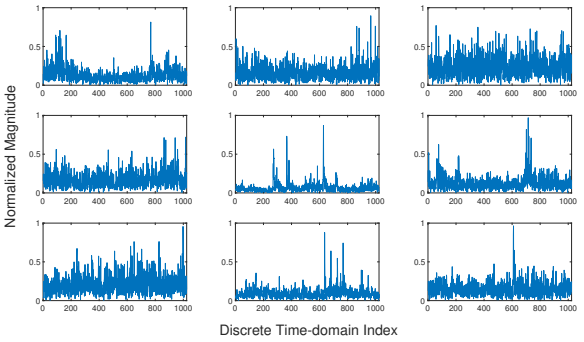

(a)

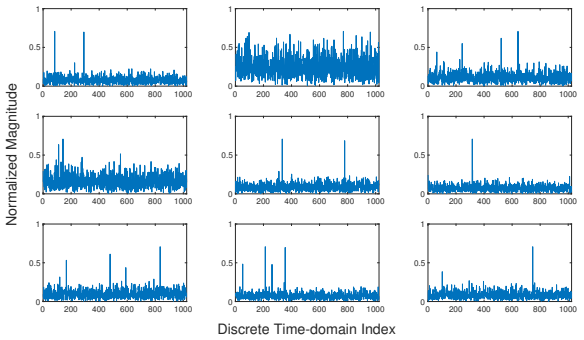

(b)

Fig. 5: HF Ship-radiated noise samples (a) real data examples, and (b) fake data examples generated via the HF GMM.

real and fake data examples [22].

2) Noise estimation and cancellation analysis via Gaussian mixture generalized approximate message passing (GM-GAMP) [8] on the ONC shipping noise, GMM generated shipping noise, and DCGAN generated shipping noise.
3) Empirical symbol error rate (SER) versus signal to noise ratio (SNR) analysis of a quadrature phase shift keying (QPSK) OFDM system without noise cancellation, imposing ship-radiated noise vectors from the ONC shipping noise, DCGAN generated shipping noise, and GMM generated shipping noise.

A. Training and Testing Data

We use the ONC ship-radiated noise data to train DCGAN models and GMMs for both the HF and LF band systems. The HF and LF ONC data sets are partitioned and normalized between $[-1,\ 1]$. The overall HF train and test set sizes are 23040 and 5760, respectively. The LF data set is lesser in size compared to the HF data set, thus we include one-dimensional translation augmented versions of the pre-processed shipping noise signals to increase the LF data set size by a factor of 4. The LF train and test set sizes are 51321 and 5703, respectively.

We use the experimental ship-radiated noise recordings as an additional test data set, which is acquired under different conditions relative the ONC shipping noise data. Because the quantity of examples of the experimentally acquired ship-radiated noise test data is significantly lesser compared to the ONC data, we only use the experimental shipping noise data for further evaluation of the 1-NN test, which requires less data examples relative to the other evaluations considered in this paper. The experimental data and the ONC test data have no influence on the training stages of the DCGAN and GMM models.

Both the HF and LF DCGAN models are trained using the Adam optimizer [23] with a mini-batch size of 128 training examples over a training period of 100 epochs with the HF and LF ONC training data sets, respectively. We use a learning rate of 0.0001 for both the generator and discriminator networks. To fit the HF and LF GMMs, we first estimate the respective GMM parameters via the EM algorithm for each shipping noise vector from the respective HF and LF training sets. Then, we take the medians of the respective EM estimated GMM component parameters of the shipping noise signals. This produces a HF and LF GMM with fixed parameters that approximates the distribution of the ship-radiated noise training data as a single two component Gaussian mixture for the HF and LF ONC data sets, respectively.

Examples of LF real ship-radiated noise signals and fake generated ship-radiated noise signals via the DCGAN model are shown in Fig 4 (a) and Fig 4 (b), respectively. Likewise,

Fig 5 (a) and Fig 5 (b) present the HF real ship-radiated noise signals and the fake GMM generated ship-radiated noise signals, respectively. From initial observation of the generated shipping noise signals shown in Fig 4 and Fig 5, it is visible that the LF DCGAN model is able to capture some of the correlative structure present in LF ship-radiated noise while the HF GMM serves well in approximating the impulsive behaviour of HF ship-radiated noise.

B. The 1-NN Two Sample Test

The 1-NN test is a type of two sample test, used to assess whether or not two distributions match. The 1-NN two sample test has been found to be an effective evaluation metric for GAN models [22]. For the purpose of our evaluation, we take advantage of the 1-NN test to provide initial observations and comments regarding the trained DCGAN models and to observe how the DCGAN models generalize to experimental shipping noise data. We report the LOO of the 1-NN test on the separated HF and LF ONC test data set and on the experimentally acquired data. Below, we denote and outline the general structure of the 1-NN two sample test.

We define $\boldsymbol{X}_{test}$ and $\boldsymbol{X}_{gen}$ as $K \times N$ matrices containing K real ship-radiated noise examples from the test set and generated ship-radiated noise examples, respectively. Here, K denotes the number of generated and real ship-radiated noise examples and N denotes the size of each example. $\boldsymbol{X}_{data} = \left[\boldsymbol{X}_{test}^T \mid \boldsymbol{X}_{gen}^T\right]^T$ is the $2K \times N$ real and generated concatenated shipping noise example matrix. Likewise, we denote $\boldsymbol{Y}_{data}$ as the $2K \times 1$ label matrix, labelling the real ship-radiated noise signals as 1 and the fake ship-radiated noise signals as -1. We shuffle the rows of $\boldsymbol{X}_{data}$ and $\boldsymbol{Y}_{data}$ synchronously. Then, we fit a 1-NN classifier using all, except for one, examples and respective labels from $\boldsymbol{X}_{data}$ and $\boldsymbol{Y}_{data}$. The single left out example, and respective label, is used in the testing stage of the previously fit 1-NN classifier. We record predicted label of the 1-NN test via the single left out example from $\boldsymbol{X}_{data}$ and the corresponding true label from $\boldsymbol{Y}_{data}$. This process is then repeated until a 1-NN classifier is fit and predicted for all $2K$ examples in $\boldsymbol{X}_{data}$. Finally, the LOO accuracy is calculated using the subsequent predicted and true labels from the $2K$ 1-NN classifiers. In this test, a LOO accuracy of 50% indicates that the 1-NN classifier cannot distinguish whether a certain example is real or fake, suggesting that the generative model well approximates the real data distribution.

We implement the 1-NN two sample test on the individual complex discrete sample points of the ship-radiated noise signals. On the ONC test data set, the $\boldsymbol{X}_{test}$ matrix is 10240×2, containing the real and imaginary components of the 10 randomly selected and concatenated actual ship-radiated noise signals. Likewise, $\boldsymbol{X}_{gen}$ is a 10240×2 matrix, containing the real and imaginary components of 10 generated and concatenated fake ship-radiated noise signals. Because the experimental data sets are significantly smaller than the ONC test data sets, we use 5 randomly selected, and 5 generated, ship-radiated noise signals for the 1-NN evaluation on the experimental data. Table III reports the LOO accuracy of the 1-NN two samples tests on the HF and LF ONC and experimental shipping noise data. From Table III it is clear that the LF DCGAN model generates samples closer to the distribution of the real data compared to the HF DCGAN model, for both the ONC and experimental shipping noise signals. Likewise, the 1-NN two sample test on the ONC and experimental data yield similar LOO accuracy results, suggesting the ONC trained DCGAN models generate shipping noise samples that to some degree represent the experimental shipping noise signals. However, apart from initial observations regarding the ability of the DCGAN model to approximate the distribution of the ship-radiated noise data, the 1-NN test does not serve as an absolute evaluation metric.

TABLE III: Per-complex-discrete sample LOO Accuracy of 1-NN Classifier For Classification of Real and Fake Data Examples on ONC test data and Experimental Data

Ship Noise Data set	DCGAN	
	Real	Fake
HF-ONC	0.609	0.612
LF-ONC	0.531	0.527
HF-EXP1	0.624	0.625
HF-EXP2	0.623	0.620
LF-EXP1	0.523	0.524
LF-EXP2	0.529	0.527

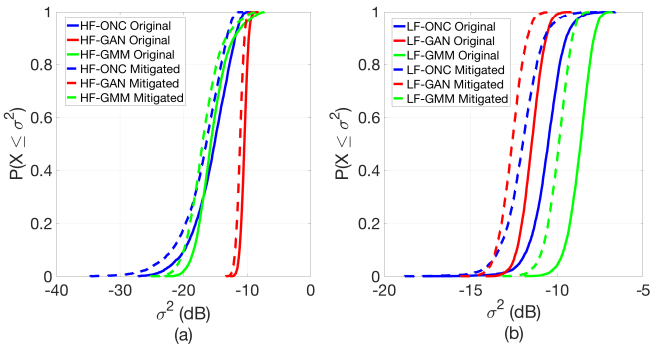

Fig. 6: CDF plot of per-OFDM symbol GM-GAMP noise cancellation results for (a) HF ship-radiated channel noise (b) LF ship-radiated channel noise.

C. Acoustic Shipping Noise Suppression Analysis

We perform noise estimation and cancellation analysis using actual ship-radiated noise signals and fake GMM and DCGAN generated ship-radiated noise signals for the HF and LF band systems. Similar to [8], we plot the empirical cumulative distribution functions (CDFs) of the per-OFDM symbol noise variance of the original and mitigated ship-radiated noise signals. The GM-GAMP algorithm for the estimation and cancellation of the real and generated ship-radiated noise signals is considered for the extent of this evaluation. For both the HF and LF band systems, we randomly select 8000 real shipping noise signals from the respective ONC training

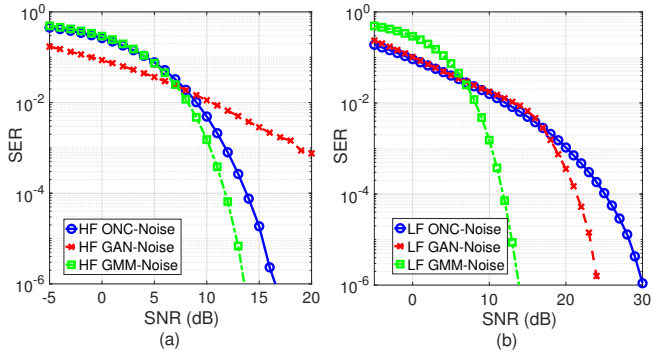

Fig. 7: SER v.s. SNR for QPSK-OFDM system in (a) HF ship-radiated channel noise (b) LF ship-radiated channel noise.

sets and generated 8000 fake shipping noise signals via the GMM and DCGAN generative models. Then, we apply the GM-GAMP algorithm to estimate and cancel the respective HF and LF actual and model generated ship-radiated noise signals.

Fig 6 (a) and Fig 6 (b) show the empirical CDF plots of the original and mitigated per-OFDM symbol shipping noise signal variances for the ONC shipping noise data, GMM generated shipping noise data, and DCGAN generated shipping noise data. With reference to Fig 6, it is clear that the GMM model provides more accurate approximation of the per-OFDM symbol ship-radiated noise variance compared to the DCGAN for the HF band system. In contrast. the DCGAN yields more realistic approximation of the per-OFDM symbol ship-radiated noise variance compared to the GMM for the LF band system. This result is consistent with our expectation that the LF ship-radiated noise carries increased correlative structure that is arguably well captured by the convolutional layers of the DCGAN. On the other hand, the GMM serves better in probabilistically modelling the impulsive attributes of HF ship-radiated noise of which the convolutional layers of the DCGAN struggle to capture.

D. OFDM System Simulation

To evaluate the effectiveness of the GMM and DCGAN in generating realistic realizations of ship-radiated noise for HF and LF OFDM systems, we report the SER versus SNR under a QPSK-OFDM system simulation framework. The closer the match between the SER curves pertaining to the QPSK-OFDM system simulation using the actual versus generated shipping noise interference, the more suitable the respective generative model in approximating the ship-radiated noise. We use ship-radiated noise samples from the ONC training set in order to observes how well the respective generative models approximate the probabilistic distributions of the training data.

We simulate a QPSK-OFDM system in the complex base-band and consider the case where all 1024 OFDM sub-carrier are utilized for data transmission. Likewise, we consider a simple OFDM system with no cyclic pre-fix and no channel estimation and equalization as we aim to only explore the additive interfering effects of ship-radiated noise. The complex QPSK modulated symbols are randomly generated from the set of points defined in $\{\pm 1,\ \pm 1\}$ and placed at the 1024 OFDM data sub-carriers. Following the IDFT of the OFDM sub-carriers, as defined in equation (1), we impose the respective ship-radiated noise signals to the time-domain OFDM signal. Then, we perform the reception process via the DFT of the time-domain OFDM signal, now containing the additive ship-radiated noise interference. We then evaluate the SER of the QPSK symbols. This process is performed and repeated over 8000 OFDM transmissions at various SNRs for the HF and LF band systems (outlined in Table I).

Fig 7 (a) and Fig 7 (b) show the SER versus SNR curves for the HF and LF OFDM systems, respectively. With reference to Fig 7 (a), it is clearly visible that the GMM serves as a more suitable time-domain stochastic model for HF ship-radiated noise in the SNR range between -5 dB to 15 dB, relative to the DCGAN. Likewise, from Fig 7 (b), we observe the DCGAN serves as a more suitable time-domain stochastic model for LF ship-radiated noise in the SNR range between -5 dB to 20 dB, compared to the GMM. Overall, these results are consistent with our expectations and indicate that the DCGAN well captures the correlative structure present in LF ship-radiated noise while the GMM is better suited in modelling the impulsive agitations which occur in the presence of HF ship-radiated noise.

V. Conclusion

In this paper we introduced the DCGAN model for modelling the time-domain stochastic behaviour of ship-radiated noise. In particular, we took advantage of convolutional layers of the DCGAN to capture the correlative structure of LF ship-radiated noise while further evaluating the GMM as a HF ship-radiated noise model. The results suggest the DCGAN model serves as a more suitable choice for modelling the time-domain stochastic behaviour of LF ship-radiated noise. This is expected as the convolutional layers of the DCGAN model are able to capture the increased correlative structure present in LF ship-radiated noise. In contrast, the GMM serves as a more suitable choice for modelling the time-domain stochastic behaviour of HF ship-radiated noise. Therefore, when evaluating the performance of UA OFDM systems in the presence of ship-radiated noise, the GMM and DCGAN generative models produce relatively accurate approximations of simulated ship-radiated noise for HF and LF band systems, respectively.

Acknowledgment

The authors would like to thank Ocean Networks Canada for providing the shipping noise data and accompanying help in using it.

References

[1] M. Stojanovic and J. Preisig, "Underwater acoustic communication channels: Propagation models and statistical characterization," *IEEE Communications Magazine*, vol. 47, no. 1, pp. 84–89, 2009.

[2] M. F. McKenna, D. Ross, S. M. Wiggins, and J. A. Hildebrand, "Underwater radiated noise from modern commercial ships," *The Journal of the Acoustical Society of America*, vol. 131, no. 1, pp. 92–103, 2012.

[3] S. Li, D. Yang, and H. Zhang, "Experimental study of underwater propeller low-frequency noise flied," in *Proceedings of China Ocean Acoustics*. IEEE, 2016, pp. 1–4.

[4] F. Traverso, T. Gaggero, E. Rizzuto, and A. Trucco, "Spectral analysis of the underwater acoustic noise radiated by ships with controllable pitch propellers," in *Proceedings of OCEANS-Genova*. IEEE, 2015, pp. 1–6.

[5] C. Pradhan and A. Gupta, "Modeling of ambient and ship noise in underwater ocean environment of the Bay of Bengal," in *Proceedings of the International Conference on Signal Processing, Informatics, Communication and Energy Systems*. IEEE, 2015, pp. 1–5.

[6] A. N. Kawade, V. M. Shinde, R. K. Shastri, and A. Das, "Analysis of ship noise from underwater ambient noise," in *Proceeding of the Conference on Advances in Signal Processing*. IEEE, 2016, pp. 265–269.

[7] S. Banerjee and M. Agrawal, "On the performance of underwater communication system in noise with gaussian mixture statistics," in *Proceedings of The Twentieth National Conference on Communications*. IEEE, 2014, pp. 1–6.

[8] L. Atanackovic, R. Zhang, L. Lampe, and R. Diamant, "Statistical shipping noise characterization and mitigation for underwater acoustic communications," in *Proceedings of OCEANS-Marseille*. IEEE, 2019, pp. 1–7.

[9] K. P. Murphy, *Machine learning: a probabilistic perspective*. MIT press, 2012.

[10] I. Goodfellow, J. Pouget-Abadie, M. Mirza, B. Xu, D. Warde-Farley, S. Ozair, A. Courville, and Y. Bengio, "Generative adversarial nets," in *Proceeding of Advances in neural information processing systems*, 2014, pp. 2672–2680.

[11] A. Radford, L. Metz, and S. Chintala, "Unsupervised representation learning with deep convolutional generative adversarial networks," *arXiv preprint arXiv:1511.06434*, 2015.

[12] M. Mirza and S. Osindero, "Conditional generative adversarial nets," *arXiv preprint arXiv:1411.1784*, 2014.

[13] H. Zhang, T. Xu, H. Li, S. Zhang, X. Wang, X. Huang, and D. N. Metaxas, "Stackgan: Text to photo-realistic image synthesis with stacked generative adversarial networks," in *Proceedings of the IEEE international conference on computer vision*, 2017, pp. 5907–5915.

[14] H. Ye, G. Y. Li, B.-H. F. Juang, and K. Sivanesan, "Channel agnostic end-to-end learning based communication systems with conditional GAN," in *Proceedings of Globecom Workshops*. IEEE, 2018, pp. 1–5.

[15] T. J. O'Shea, T. Roy, and N. West, "Approximating the void: Learning stochastic channel models from observation with variational generative adversarial networks," in *Proceedings of the International Conference on Computing, Networking and Communications*. IEEE, 2019, pp. 681–686.

[16] X. Yao, H. Yang, and Y. Li, "Modulation identification of underwater acoustic communications signals based on generative adversarial networks," in *Proceedings of OCEANS-Marseille*. IEEE, 2019, pp. 1–6.

[17] G. Jin, F. Liu, H. Wu, and Q. Song, "Deep learning-based framework for expansion, recognition and classification of underwater acoustic signal," *Journal of Experimental & Theoretical Artificial Intelligence*, vol. 32, no. 2, pp. 205–218, 2020.

[18] M. Sung, H. Cho, J. Kim, and S.-C. Yu, "Sonar image translation using generative adversarial network for underwater object recognition," in *Proceedings of IEEE Underwater Technology*. IEEE, 2019, pp. 1–6.

[19] M. Sung, J. Kim, and S.-C. Yu, "Image-based super resolution of underwater sonar images using generative adversarial network," in *Proceedings of TENCON*. IEEE, 2018, pp. 0457–0461.

[20] Ocean Networks Canada, "Search hydrophone data," January 2016, https://data.oceannetworks.ca/SearchHydrophoneData.

[21] C. Trabelsi, O. Bilaniuk, Y. Zhang, D. Serdyuk, S. Subramanian, J. F. Santos, S. Mehri, N. Rostamzadeh, Y. Bengio, and C. Pal, "Deep complex networks," in *Proceedings of the International Conference on Learning Representations*, 2018.

[22] Q. Xu, G. Huang, Y. Yuan, C. Guo, Y. Sun, F. Wu, and K. Weinberger, "An empirical study on evaluation metrics of generative adversarial networks," *arXiv preprint arXiv:1806.07755*, 2018.

[23] D. P. Kingma and J. Ba, "Adam: A method for stochastic optimization," *arXiv preprint arXiv:1412.6980*, 2014.